HHS Public Access

Author manuscript

Proteomics Clin Appl. Author manuscript; available in PMC 2024 November 01.

Published in final edited form as:

Proteomics Clin Appl. 2023 November ; 17(6): e2200109. doi:10.1002/prca.202200109.

Valosin-Containing Protein (VCP/p97) is Prognostically Unfavorable in Pediatric AML, and Negatively Correlates with Unfolded Protein Response Proteins IRE1 and GRP78: a Report from the Children's Oncology Group

Fieke W. Hoff[1], **Yihua Qiu**[2], **Brandon D. Brown**[3], **Robert B. Gerbing**[4], **Amanda R. Leonti**[5], **Rhonda E. Ries**[5], **Alan S. Gamis**[6], **Richard Aplenc**[7], **E. Anders Kolb**[8], **Todd A. Alonzo**[4,9], **Soheil Meshinchi**[5], **Gaye N Jenkins**[10], **Terzah Horton**[10,*], **Steven M. Kornblau**[2,*]

[1]Department of Internal Medicine, University of Texas Southwestern Medical Center, Dallas, TX, USA

[2]Department of Leukemia, The University of Texas MD Anderson Cancer Center, Houston, TX

[3]Department of Pediatrics, The University of Texas MD Anderson Cancer Center, Houston, TX

[4]COG Statistics and Data Center, Monrovia, CA

[5]Clinical Research Division, Fred Hutchinson Cancer Research Center, Seattle, Washington, USA

[6]Department of Hematology-Oncology, Children's Mercy Hospitals and Clinics, Kansas City, MO

[7]Division of Pediatric Oncology/Stem Cell Transplant, Children's Hospital of Philadelphia, Philadelphia, PA

[8]Nemours Center for Cancer and Blood Disorders, Alfred I. DuPont Hospital for Children, Wilmington, DE

[9]Keck School of Medicine, University of Southern California, CA

[10]Department of Pediatrics, Baylor College of Medicine/Dan L. Duncan Cancer Center and Texas Children's Cancer Center, Houston, Texas

Abstract

Purpose: The endoplasmic reticulum (ER) is the major site of protein synthesis and folding in the cell. ER-associated degradation (ERAD) and unfolded protein response (UPR) are the

Corresponding author: Steven M. Kornblau, Address: 1515 Holcombe Blvd, Box 448, Houston, Texas 77030-4009, Phone: 713-794-1568, Fax: 713-794-1938, skornblau@mdanderson.org.

*Contributed equally to the work; Co-senior authors.

Author Contributions

The following are responsible for the work done in this manuscript. FWH, TMH, SMK designed and supervised the research, FWH, YQ, GNJ, TMH, SMK performed the research, YQ, ASG, RA, EAK, TAA, TMH, SMK collected data, FWH, BDB, RBG, ARL, RER, SM, TMH, SMK analyzed data, and FWH, TMH, SMK wrote the paper.

Conflict of interest statement

TMH receives research funding from Takeda Pharmaceuticals.

Declaration

The content is solely the responsibility of the authors and does not necessarily represent the official views of the National Institutes of Health.

main mechanisms of ER-mediated cell stress adaptation. Targeting the cell stress response is a promising therapeutic approach in acute myeloid leukemia (AML).

Experimental design: Protein expression levels of VCP, a chief element of ERAD, were measured in peripheral blood samples from in 483 pediatric AML patients using reverse phase protein array methodology. Patients participated in the Children's Oncology Group AAML1031 phase 3 clinical trial that randomized patients to standard chemotherapy (cytarabine (Ara-C), daunorubicin, and etoposide [ADE]) vs ADE plus bortezomib (ADE+BTZ).

Results: Low-VCP expression was significantly associated with favorable 5-year overall survival (OS) rate compared to middle-high-VCP expression (81% vs 63%, $p<0.001$), independent of additional bortezomib treatment. Multivariable Cox regression analysis identified VCP as independent predictor of clinical outcome. UPR proteins IRE1 and GRP78 had significant negative correlation with VCP. Five-year OS in patients characterized by low-VCP, moderately high-IRE1 and high-GRP78 improved after treatment with ADE+BTZ vs ADE (66% vs 88%, $p=0.026$).

Conclusion and clinical relevance: Our findings suggest the potential of the protein VCP as biomarker in prognostication prediction in pediatric AML.

Keywords

VCP; IRE1; GRP78; UPR; ERAD; leukemia; AML; RPPA; pediatric

Introduction

The endoplasmic reticulum (ER) is the major site of protein synthesis and protein folding in the cell. Three pathways are integrated to maintain ER homeostasis: ER-associated degradation (ERAD), unfolded protein response (UPR), and autophagy. Whereas ERAD is responsible for retrograde translocation of misfolded proteins to the cytoplasm from the ER for proteasomal degradation, the UPR is activated in response the accumulation of misfolded proteins arising from a failure in protein clearance, resulting in a pause in protein synthesis, and over time, in apoptosis. [1] One of the chief elements of ERAD is the highly conserved type II AAA-ATPase superfamily member valosin-containing protein (VCP), also known as p97. Various studies have reported an upregulation of VCP in cancer, including breast and gastric carcinoma, and an association between elevated VCP expression and unfavorable cancer outcome. [2–6]

VCP forms a hexameric, ring-shaped complex of subunits that consist of a N-terminal domain which enables recognition of the substrate and interacts with other cofactors (e.g., Ufd1, Np14). There are two D-domains responsible for ATPase activity and a C-terminus that is involved in nuclear localization by binding with other proteins. [6–8] VCP is tightly regulated by numerous cofactors, including the group of ubiquitin regulatory X (UBX) proteins. [9,10] VCP uses the energy of ATP hydrolysis to change its structure, which facilitates the degradation of its targets, including polyubiquitylated substrates. Proteolysis-independent functions of VCP have also been described including cell cycle progression, transcriptional activation, and DNA damage repair, all with the common underlying function

to extract ubiquitylated substrate proteins from large protein assemblies or immobile cellular structures. [7,8,10]

Pediatric acute myeloid leukemia (AML) has a guarded prognosis. Decades of effort have improved our understand of the underlying biology and have improved outcome. However, 5-year (year) overall survival (OS) rates remain 60–70% in the pediatric population, pointing out the urgent need for more efficacious, well-tolerated, therapeutic strategies. [11–16] With varying degrees of success, targeted therapeutics, epigenetic modifiers, immune-based strategies, and novel metabolic pathway inhibition have all been investigated in adult AML, and to a certain extent in pediatric AML. Targeting the cellular stress response is another promising target, which is currently in early-phase clinical trials in adults. Systemic functional genomic screens have identified VCP as a potential target for inhibition in AML, and found that AML was the most responsive disease to chemical inhibition of VCP across a panel of 16 cancer types. [17] CB-5339 is a potent and selective second-generation oral small molecule inhibitor of VCP that is currently being evaluated in a Phase I clinical trial of adults with relapsed/ refractory AML and myelodysplastic syndrome. [18] As the clinical impact of VCP has not been studied in pediatric AML, we examined relative VCP protein expression levels at time of diagnosis to determine if they were predictive of outcome in pediatric AML.

Materials and methods

Patient samples

Peripheral blood samples from 483 *de novo* pediatric AML patients were collected between July 2011 and February 2017 during diagnostic assessments prior to the start of chemotherapy. Patients participated in the Children's Oncology Group AAML1031 Phase 3 clinical trial, that randomized patients to either standard of care (cytarabine (AraC), daunorubicin, etoposide [ADE]) or standard of care plus the proteasome inhibitor bortezomib (ADE+BTZ). Written informed consent was obtained in accordance with *Declaration of Helsinki*. Patient characteristics are shown in Table 1.

Sample processing

Fresh AML samples were shipped to a central laboratory and isolated by centrifugation using lymphocyte separation solution (Sigma), then enriched for AML myeloblasts using CD3/CD19 magnetic beads to deplete T and B cells (Miltenyi Biotech, Cologne, Germany). Cells were lysed into a total protein lysis solution (Biorad) and protein preparations were normalized to a concentration of 10,000 cells/μL before freezing at −80 °C.

RPPA methodology

The methodology and validation of the RPPA technique are fully described elsewhere. [19–23] Briefly, whole cell protein lysates were printed in five serial 1:2 dilutions onto slides along with normalization and expression controls. Slides were probed with 296 antibodies listed in Supplemental Table S1, including a primary validated antibody against VCP (#11433, Abcam, Cambridge, UK), IRE1 (#3294, Cell signaling Technology, Danvers, MA), and GRP78 (#610978, BD Biosciences, San Jose, CA). Stained slides were analyzed using

Microvigene® Software (version 3.0, Vigene Tech, Carlisle, MA). *SuperCurve* algorithms were used to generate a single value of protein expression from the five serial dilutions. [24] Loading control [25] and topographical normalization [26] procedures were performed to account for protein concentration and background staining variations on each array. Replicate-based normalization was used to align samples from two different slides. [27] Overlapping samples (n=98) between the two slides had an average Pearson's correlation coefficient of 0.88. For each protein, the median expression levels of normal pediatric BM CD34+ samples (n=20)) were subtracted from the expression in the patient samples to obtain relative protein expression.

Transcriptome sequencing data

Ribodepleted RNA-sequencing data for 58263 genes was generated for the AAML1031 patient samples as described elsewhere. [28] Data was available for 397 of the 483 patients. Messenger RNA-sequencing reads were aligned to the GRCh38 reference genome and normalized in transcripts per million. Mutation profiles were obtained from transcriptome sequencing data. Mutations present in ≥ 10 patients included: NRAS (n=99), KRAS (n=29), PTPN11 (n=28), MYH11 (n=17), IDH1 or IDH2 (n=14), and GATA2 (n=12)).

miRNA sequencing

miRNA sequencing was performed as previously published and data was obtained from Bolouri et al. [29–32] miRNA-sequencing reads were aligned to the GRCh37-lite reference genome and annotated using mirBase v21 annotations. Expression was normalized to reads per million. Integrative miRNA:mRNA analysis was performed as previously described.[32] Only samples for which there was both miRNA-seq and mRNA-seq data (n=164) were considered. Briefly, a Spearman correlation coefficient score and a p-value were generated for comparisons of expression profiles between all possible miRNA and mRNA pairs. Then, miRNA:mRNA pairs were shortlisted based on the presence of target site predictions (from both TargetScan and miRanda algorithms [33,34]) and significant anti-correlation between miRNA and gene expression, with statistical significance determined by comparison against bootstrapping-based null distributions.

Statistical analysis

Estimates of OS and event-free survival (EFS) were calculated using the Kaplan–Meier method. OS and EFS were defined as time from study entry until relapse, secondary malignancy or death, respectively. Relapse risk (RR) was calculated using methods of competing events and was defined as the time from the end of two courses of induction (for patients in complete remission) to relapse, where deaths without a relapse were considered competing events. Estimates are reported with log-log 95% confidence intervals. Differences between groups of patients were tested for significance using the log-rank statistic for OS and EFS. Gray's test was used to test significance for RR. Cox regression was performed for multivariable analyses of OS and EFS, whereas, competing risk regression was used for multivariable analyses of RR.

Patients were divided into three cohorts based on their relative VCP RPPA protein expression. Proportions between the clusters and categorical clinical variables were

compared using Pearson's Chi-square test. Pearson's correlation analyses were performed to investigate correlation between VCP protein expression levels and the other proteins assessed on the RPPA, as well as between protein and mRNA expression levels. *P*-values were adjusted using FDR correction. Differentially expressed miRNAs and mRNAs were determined using differential analysis of count data. [35] Gene ontology pathway analysis was performed on the differentially expressed genes. [36] All statistical analyses were performed in R (Version 0.99.484 –2009–2015 RStudio, Inc.) or SAS (version 9.4).

Results

VCP is expressed within the range of normal CD34+ cells

Relative VCP expression was measured in CD3/CD19 depleted cells obtained from 483 pediatric AML patients and compared to expression in 20 normal pediatric CD34+ cells. Overall, expression was comparable in AML and normal CD34+ cells (p=0.85) (Supplemental Figure S1A). Eleven percent of the AML patients had relative expression higher than the 95% CI upper limit of the healthy donors and 6% lower than the 95% CI lower limit.

Higher VCP expression in high-risk cytogenetics and mutations

VCP levels were correlated with individual cytogenetic abnormalities and mutational status. VCP was lower in low-risk cytogenetics associated with core binding factor AML (inv (16) ($p<0.001$), t (8;21)) ($p<0.001$), as well as in mutated KIT (both exon 8 and 17) ($p<0.001$) and mutated MYH11 ($p<0.001$). Significantly higher VCP levels were seen in KMT2A-rearranged AML (MLL) ($p<0.001$) and in patients with FLT3-ITD mutation (p=0.047) (Figure 1A–G). CEBPA, NPM1, KRAS, NRAS, PTPN11, IDH1, IDH2, and GATA2 mutation status were not associated with VCP protein expression, nor was FAB classification (Supplemental Figure S1B–H). In addition, VCP was more highly expressed in infants (age ≤1 year at diagnosis) (p=0.032) and in patients with higher white blood cell counts (p=0.016) (Figure 1H–I). No difference in VCP expression was seen for gender, race, ethnicity, and CNS leukemia status (Supplemental Figure S1I–L).

Low-VCP protein levels are prognostically favorable in pediatric AML, independent of treatment

Outcome data were available for 410 of the patients enrolled on the AAML1031 study. Data were frozen as of June 30, 2022, with a median follow-up period of 6.4 years (range 0.3–10.2 years). One hundred and sixty-four patients received standard ADE induction therapy, 210 patients received ADE in combination with BTZ, and 36, with known FLT3-ITD mutations, received ADE + sorafenib (ADE+S) starting on Day 15 of induction. Three hundred forty-eight (85%) patients achieved CR by the end of course 2, 31 (7.6%) patients were refractory or died (failed therapy). One hundred sixty (46%) patients relapsed or died after remission, and 285 were still alive at the end of their follow-up (70%).

Based on the preliminary evidence that VCP-inhibition may work as a treatment for AML, [17,18] we wondered whether lower baseline VCP expression was associated with better outcome in pediatric AML. Because we found that relative VCP expression, divided into

sextiles (Supplemental Figure S2), was significantly prognostic, with the first two sextiles being strongly associated with better clinical outcome, patients were stratified into three groups; low vs middle vs high-VCP expression. As outcome data was available for 410/483 patient, OS analysis revealed a 5-year OS of 81% (95% CI: 73%–87%) in the low-VCP group (n=128) vs 63% (95% CI: 57%–69%) in the middle to high-VCP patients (n=282) ($p<0.001$) from study entry. A similar observation was found for EFS (5-year EFS, 59% (95% CI: 50%–67%) vs 46% (95% CI: 40%–52%), p=0.003) and RR (5-year RR, 34% (95% CI: 25%–43%) vs 44% (95% CI: 37%–50%), p=0.017) (Figure 2A–C). Consistently, low-VCP had a favorable prognosis within the low-risk AML patients (inv(16)/t(16;16) or t(8;21), or NPM1 or CEBPα mutation) (Supplemental Figure S3A, OS, p=0.006). Within the high-risk patients, defined per AAML1031 risk-protocol, VCP was not prognostic for OS, EFS or RR (OS, p=0.081; EFS, p=0.579 (not shown); RR, p=0.663, Supplemental Figure S3B–C).

As VCP plays a critical role in the ERAD, we asked whether the prognostic impact of VCP was affected by the proteosome inhibitor bortezomib, which interferes with the UPR and ERAD by inhibiting the proteasome. We compared the outcomes of patients who received standard therapy with ADE vs those that received ADE+BTZ. Within each level of VCP expression (low-VCP, middle-VCP, high-VCP), patients that received bortezomib had a similar outcome compared to those that did not (Supplemental Figure S3D–F).

When multivariable analysis was performed including risk groups stratified based on the AAML1031 risk definition groups, both cytogenetic risk groups, age and VCP remained independently prognostic for OS and EFS, with high-VCP and age ≤ 1 being independently prognostic for relapse risk (Table 2).

VCP expression remains stable after exposure to treatment

To assess the effect of treatment on VCP expression, leukemia cells were collected prior to, 10 and 24 hours after exposure to treatment from paired patient samples. Overall, VCP remained stable without significant increase or decrease in expression after 10 or 24 hours (p=0.76, p=0.33, respectively) (Figure 3A), both after ADE and ADE+BTZ treatment. Similar findings were found when we separately looked at patients with low, middle or high-VCP baseline expression levels (data not shown).

VCP negatively correlates with unfolded protein response proteins IRE1 and GRP78

Two major protein stress response pathways in AML are the ERAD (with VCP as an important component, upstream of the proteasome) and the UPR (with Glucose Regulating Protein 78 (GRP78) and ER-resident transmembrane Inositol-Requiring Enzyme 1 (IRE1, HUGO name ERN1) as important components). We correlated expression of VCP with two UPR proteins IRE1 and GRP78 (the main UPR sensor of ER stress), and found a significant negative correlation with both GRP78 ($r=-0.23$, $p<0.001$) and IRE1 ($r=-030$, $p<0.001$) (Supplemental Figure S4A–B). Clustering analysis of the pediatric AML patient samples for VCP, IRE1 and GRP78 identified four proteins clusters (Figure 3B). In line with our findings that low-VCP is favorably prognostic, survival analysis showed better outcome associated within cluster 1 and 2, both characterized by low-VCP vs cluster 3

and 4 characterized by moderate/ high-VCP (Figure 3C, upper panel). When outcome was assessed in the context of ADE and ADE+BTZ treatment, however, outcome in cluster 2 significantly improved with the addition of bortezomib (Figure 3C, lower panel), whereas cluster 1 tended to do more poorly. Protein cluster 2 (pink) was characterized by highest relative GRP78 levels combined with moderately high IRE1. Notably, while high-GRP78 individually was also associated with better response to bortezomib (64% (95% CI: 53% −72%) vs 80% (95% CI: 71%−87%) OS-rate at 5-year) (Supplemental Figure S5), the combination of low-VCP, modest-IRE1 and high-GRP78 was more strongly associated with improvement of OS and EFS when treated with ADE+BTZ (66% (95% CI: 50%−78%) vs 88% (95% CI: 71%−95%) OS-rate at 5-year) (Figure 3C, lower panel) (p=0.026).

VCP is associated with cell cycle activation, signal transduction and ribosomal synthesis

To further examine the role of VCP in pediatric AML, VCP expression levels were correlated with 295 protein targets analyzed by RPPA. Proteins with a significant absolute correlation coefficient ≥ 0.25 are shown in Figure 3D (n=137) (Supplemental Table S2). Increased VCP was positively correlated with translation/ ribosomal proteins (Figure 3D, red) EIF4EBP1, EIF4EBP1-pThr37_46 (activates translation), EIF4E, RPS6, EEF2K (which phosphorylates EEF2), and EEF2, an essential factor of protein synthesis. VCP also positively correlated with protein modifications involved in histone methylation modifying enzymes (purple asterisk), including HDAC2, HDAC6, [37] NCL and KDM1A. Signal transduction proteins both positively and negatively correlated (e.g., AKT3, TSC2-pThr and AKT1S1-pThr), inhibitory cell cycle regulators CDKN1A, E2F1 were negatively correlated, whereas phosphorylated CDKN1B and total-RB1 went up with higher VCP levels.

VCP protein expression correlated with genes involved in regulation of ubiquitin transferase activity

We wanted to study how well VCP-protein levels correlated with VCP-mRNA levels, and whether specific genes expression profiles were up-regulated in the low (favorable prognosis) vs middle and high-VCP protein expression patient subgroups. mRNA levels were available for 397 of the 483 patients and for 58263 genes. No correlation between VCP-protein expression and VCP-mRNA, VCP-interacting protein 1 (VCPIP1)-mRNA or VCP lysine methyltransferase (VCPKMT)-mRNA levels was observed (r=−0.05, r=−0.029, r=−0.072, respectively) (Supplemental Figure S6A–C). A better correlation was observed between mRNA levels of VCP and mRNA levels of VCPIP1 and VCPKMT (r=0.48 and r=0.41, respectively (p<0.001)) (Supplemental Figure S6D–E).

RNA-seq differential expression analysis including Bayesian shrinkage estimators for effect sizes, was performed resulting in 367 genes significantly differentially expressed between low-VCP vs. middle plus high-VCP grouped patients. [38] Genes were considered differentially expressed with adjusted p-value less than 0.05. Gene ontology enrichment analysis for biological processes demonstrated most fold enrichment of genes associated with regulation of ubiquitin-protein transferase activity (Figure 3E, Supplemental Table S3). Subsequently, integrative miRNA:mRNA analysis [30] using matched miRNA sequencing and mRNA sequencing data was performed to study candidate targets of miRNAs targeting

VCP mRNA. This analysis revealed 36 miRNAs with VCP as putative target (Supplemental Table S4).

Discussion

In this study we report for the first time on the prognostic significance of VCP protein expression in pediatric AML. In concordance with several other cancers, we identified low-VCP as a favorable prognostic protein for OS, EFS and relapse rate, suggesting a potential role as indicator for risk stratification. Cox regression analysis identified low-VCP as significant variable for clinical outcome in both univariable and multivariable models, suggesting that VCP is an independent predictor of outcome in pediatric AML. Despite the known role of VCP in protein homeostasis and degradation, no additional survival benefit was observed when patients expressing low pre-treatment VCP levels were treated with proteasome inhibition.

However, we observed that patients expressing low-VCP associated with moderately high-IRE1 and high-GRP78 had better clinical outcome with bortezomib, suggesting that patients that most strongly depend on the proteasome (i.e., high activity of the UPR; moderate to high IRE1, high GRP78, low activity of the ERAD; low VCP) do benefit from bortezomib addition. While AML patients with high-GRP78 had significantly improved clinical outcome after bortezomib (Supplemental Figure S3), this effect was stronger when patients with high-VCP were excluded (Figure 3C, lower panel).

Recently others showed synergistic *in vitro* effects in cells treated with CB-5083 (VCP-inhibitor) combined with standard AML therapy of cytarabine or daunorubicin, as well as with CB-5083 combined with the Bcl-2 inhibitor venetoclax. [17,39] Although the mechanism behind the effect is not fully understood, there is supporting evidence that VCP may play a role in the adaptive mechanism to cell stress. Szczęśniak et al. found that based on mass spectrometry analysis, VCP is associated with multiple components of the ubiquitin-machinery. [39] They also observed an increase in the UPR and apoptosis in AML cells that had been exposed to the VCP-inhibitor for an extended time period, including increased expression of GRP78 and IRE1. Others observed induction of the UPR, autophagy and DNA damage repair/ response upon inhibition of VCP. [17] This suggests that inhibition of VCP triggers increased cell stress resulting in activation of UPR. However, our negative correlation between VCP and IRE1 and GRP78 found in treatment-naïve cells, suggests a distinctive dependency of ERAD and UPR utilization in AML at baseline. Further research is needed in this area.

To further explore distinct VCP baseline protein levels between samples, protein levels were correlated with mRNA-expression. There was poor correlation between protein and mRNA levels, similar to what was found previously by our group and others. Given that after transcription, mRNA transcripts undergo alternative splicing, and translation, that is further affected by the miRNA that targets the gene, this lack of correlation is not surprising. We identified 36 miRNA fragments targeting the VCP gene.

This is the first study that looks at an integrated cell stress marker prior to treatment exposure, rather than after response to treatment. The advantages of this study include its large sample size and homogenously treated patient population in the setting of a clinical trial. Although the clinical trial from which the samples were obtained was a Phase 3 prospective clinical trial, the samples were analyzed retrospectively. Future studies are needed to further elucidate the *in vitro* and *in vivo* mechanistic role of VCP in AML treatment resistance. For instance, longitudinal measurements of VCP expression levels, ideally at single-cell level, can provide insight in how VCP adapts to treatment in treatment sensitive and resistant leukemia cells.

In summary, we showed the prognostic association of low-VCP with favorable outcome in pediatric AML. This suggests that VCP could be a potential marker of risk stratification.

Supplementary Material

Refer to Web version on PubMed Central for supplementary material.

Acknowledgements

A kind acknowledgment for the clerical assistance offered by Nancy Ramirez.

Financial support

TMH, RBG, ASG, RA, EAK, and RAA were funded by the NIH COG Grants U10 CA98543, U10 CA98413, U10 CA180886, U24 CA196173 and U10 CA180899. TMH was funded by the NCI R01-CA164024, a grant from, the St. Baldrick's Foundation, and a grant from Takeda Pharmaceuticals.

References

[1]. Qi L, Tsai B, Arvan P, New Insights into the Physiological Role of Endoplasmic Reticulum-Associated Degradation 2016, 27, 430–440.

[2]. Li C, Huang Y, Fan Q, Quan H, et al., p97/VCP is highly expressed in the stem-like cells of breast cancer and controls cancer stemness partly through the unfolded protein response 2021, 12, 286.

[3]. Gareau A, Rico C, Boerboom D, Nadeau M-., In vitro efficacy of a first-generation valosin-containing protein inhibitor (CB-5083) against canine lymphoma 2018, 16, 311–317.

[4]. Luo H, Song H, Mao R, Gao Q, et al., Targeting valosin-containing protein enhances the efficacy of radiation therapy in esophageal squamous cell carcinoma 2019, 110, 3464–3475.

[5]. Cui Y, Niu M, Zhang X, Zhong Z, et al., High expression of valosin-containing protein predicts poor prognosis in patients with breast carcinoma 2015, 36, 9919–9927.

[6]. Yamamoto S, Tomita Y, Aozasa K, Hoshida Y, et al., Expression Level of Valosin-Containing Protein Is Strongly Associated With Progression and Prognosis of Gastric Carcinoma 2003, 21, 2537–2544.

[7]. Sun X, Qiu H, Valosin-Containing Protein, a Calcium-Associated ATPase Protein, in Endoplasmic Reticulum and Mitochondrial Function and Its Implications for Diseases 2020, 21, 3842.

[8]. Lopata A, Kniss A, Löhr F, Rogov VV, Dötsch V, Ubiquitination in the ERAD Process 2020, 21, 5369.

[9]. Stapf C, Cartwright E, Bycroft M, Hofmann K, Buchberger A, The General Definition of the p97/Valosin-containing Protein (VCP)-interacting Motif (VIM) Delineates a New Family of p97 Cofactors 2011, 286, 38670–38678.

[10]. Schuberth C, Buchberger A, UBX domain proteins: major regulators of the AAA ATPase Cdc48/p97 2008, 65, 2360–2371.

[11]. Elgarten CW, Aplenc R, Pediatric acute myeloid leukemia: updates on biology, risk stratification, and therapy 2020, 32, 57–66.

[12]. Zwaan CM, Kolb EA, Reinhardt D, Abrahamsson J, et al., Collaborative Efforts Driving Progress in Pediatric Acute Myeloid Leukemia 2015, 33, 2949–2962.

[13]. Nunes A. de L., Paes C. de A., Murao M, Viana MB, B.M. De Oliveira, Cytogenetic abnormalities, WHO classification, and evolution of children and adolescents with acute myeloid leukemia 2019, 41, 236–243.

[14]. Moore AS, Kearns PR, Knapper S, Pearson A, Zwaan CM, Novel therapies for children with acute myeloid leukaemia 2013, 27, 1451–1460.

[15]. Pui C-H, Carroll WL, Meshinchi S, Arceci RJ, Biology, Risk Stratification, and Therapy of Pediatric Acute Leukemias: An Update 2011, 29, 551–565.

[16]. Elgarten CW, Aplenc R, Pediatric acute myeloid leukemia: updates on biology, risk stratification, and therapy 2020, 32, 57–66.

[17]. Roux B, Vaganay C, Vargas JD, Alexe G, et al., Targeting acute myeloid leukemia dependency on VCP-mediated DNA repair through a selective second-generation small-molecule inhibitor 2021, 13, 1.

[18]. Benajiba L, Carraway HE, Hamad N, Stein EM, et al., Trials in Progress: A Phase I Study to Evaluate the Safety and Pharmacokinetic Profiles of CB-5339 in Participants with Relapsed/Refractory Acute Myeloid Leukemia or Relapsed/Refractory Intermediate or High-Risk Myelodysplastic Syndrome 2020, 136, 21.

[19]. Hoff FW, van Dijk AD, Qiu Y, Ruvolo PP, et al., Heat Shock Factor 1 (HSF1-pSer326) Predicts Response to Bortezomib-Containing Chemotherapy in Pediatric AML: a COG Report 2021, 137, 1050–1060.

[20]. Kornblau SM, Tibes R, Qiu YH, Chen W, et al., Functional proteomic profiling of AML predicts response and survival 2009, 113, 154–164.

[21]. Kornblau SM, Coombes KR, Use of reverse phase protein microarrays to study protein expression in leukemia: technical and methodological lessons learned 2011, 785, 141–155.

[22]. Tibes R, Qiu Y, Lu Y, Hennessy B, et al., Reverse phase protein array: validation of a novel proteomic technology and utility for analysis of primary leukemia specimens and hematopoietic stem cells 2006, 5, 2512–2521.

[23]. Hoff FW, van Dijk AD, Qiu Y, Hu CW, et al., Clinical relevance of proteomic profiling in de novo pediatric acute myeloid leukemia: a Children's Oncology Group study 2022, 107, 2329–2343.

[24]. Hu J, He X, Baggerly KA, Coombes KR, et al., Non-parametric quantification of protein lysate arrays 2007, 23, 1986–1994.

[25]. Neeley ES, Kornblau SM, Coombes KR, Baggerly KA, Variable slope normalization of reverse phase protein arrays 2009, 25, 1384–1389.

[26]. Neeley ES, Baggerly KA, Kornblau SM, Surface Adjustment of Reverse Phase Protein Arrays using Positive Control Spots 2012, 11, 77–86.

[27]. Akbani R, Ng PK, Werner HM, Shahmoradgoli M, et al., A pan-cancer proteomic perspective on The Cancer Genome Atlas 2014, 5, 3887.

[28]. Smith JL, Ries RE, Hylkema T, Alonzo TA, et al., Comprehensive Transcriptome Profiling of Cryptic CBFA2T3–GLIS2 Fusion–Positive AML Defines Novel Therapeutic Options: A COG and TARGET Pediatric AML Study 2020, 26, 726–737.

[29]. Bolouri H, Farrar JE, Triche T Jr, Ries RE, et al., The molecular landscape of pediatric acute myeloid leukemia reveals recurrent structural alterations and age-specific mutational interactions 2018, 24, 103–112.

[30]. Lim EL, Trinh DL, Scott DW, Chu A, et al., Comprehensive miRNA sequence analysis reveals survival differences in diffuse large B-cell lymphoma patients 2015, 16, 18.

[31]. Lamble AJ, Eidenschink Brodersen L, Alonzo TA, Wang J, et al., CD123 Expression Is Associated With High-Risk Disease Characteristics in Childhood Acute Myeloid Leukemia: A Report From the Children's Oncology Group 2022, 40, 252–261.

[32]. Lim EL, Trinh DL, Ries RE, Wang J, et al., MicroRNA Expression-Based Model Indicates Event-Free Survival in Pediatric Acute Myeloid Leukemia 2017, 35, 3964–3977.

[33]. John B, Enright AJ, Aravin A, Tuschl T, et al., Human MicroRNA Targets 2004, 2, e363.

[34]. McGeary SE, Lin KS, Shi CY, Pham TM, et al., The biochemical basis of microRNA targeting efficacy 2019, 366, 1470.

[35]. Drmanac R, Sparks AB, Callow MJ, Halpern AL, et al., Human Genome Sequencing Using Unchained Base Reads on Self-Assembling DNA Nanoarrays 2010, 327, 78–81.

[36]. Huang DW, Lempicki RA, Sherman BT, Systematic and integrative analysis of large gene lists using DAVID bioinformatics resources 2008, 4, 44–57.

[37]. Li Y, Shin D, Kwon SH, Histone deacetylase 6 plays a role as a distinct regulator of diverse cellular processes 2013, 280, 775–793.

[38]. Zhu A, Ibrahim JG, Love MI, Heavy-tailed prior distributions for sequence count data: removing the noise and preserving large differences 2019, 35, 2084–2092.

[39]. Szczęśniak PP, Heidelberger JB, Serve H, Beli P, Wagner SA, VCP inhibition induces an unfolded protein response and apoptosis in human acute myeloid leukemia cells 2022, 17, e0266478. stylefix

Clinical Significance

ER-associated degradation (ERAD) and unfolded protein response (UPR) are the main mechanisms of ER-mediated cell stress adaptation. We identified valosin-containing protein (VCP) protein expression, a chief element of ERAD, as an independent unfavorably prognostic protein in pediatric acute myeloid leukemia. VCP was negative correlated with UPR proteins IRE1 and GRP78. In patients characterized by low-VCP, high-IRE1 and GRP78 overall survival at 5-years significantly improved after treatment with ADE+BTZ vs ADE alone (66% vs 88%, p=0.026). Our findings suggest the potential of VCP as biomarker in current prognostication prediction.

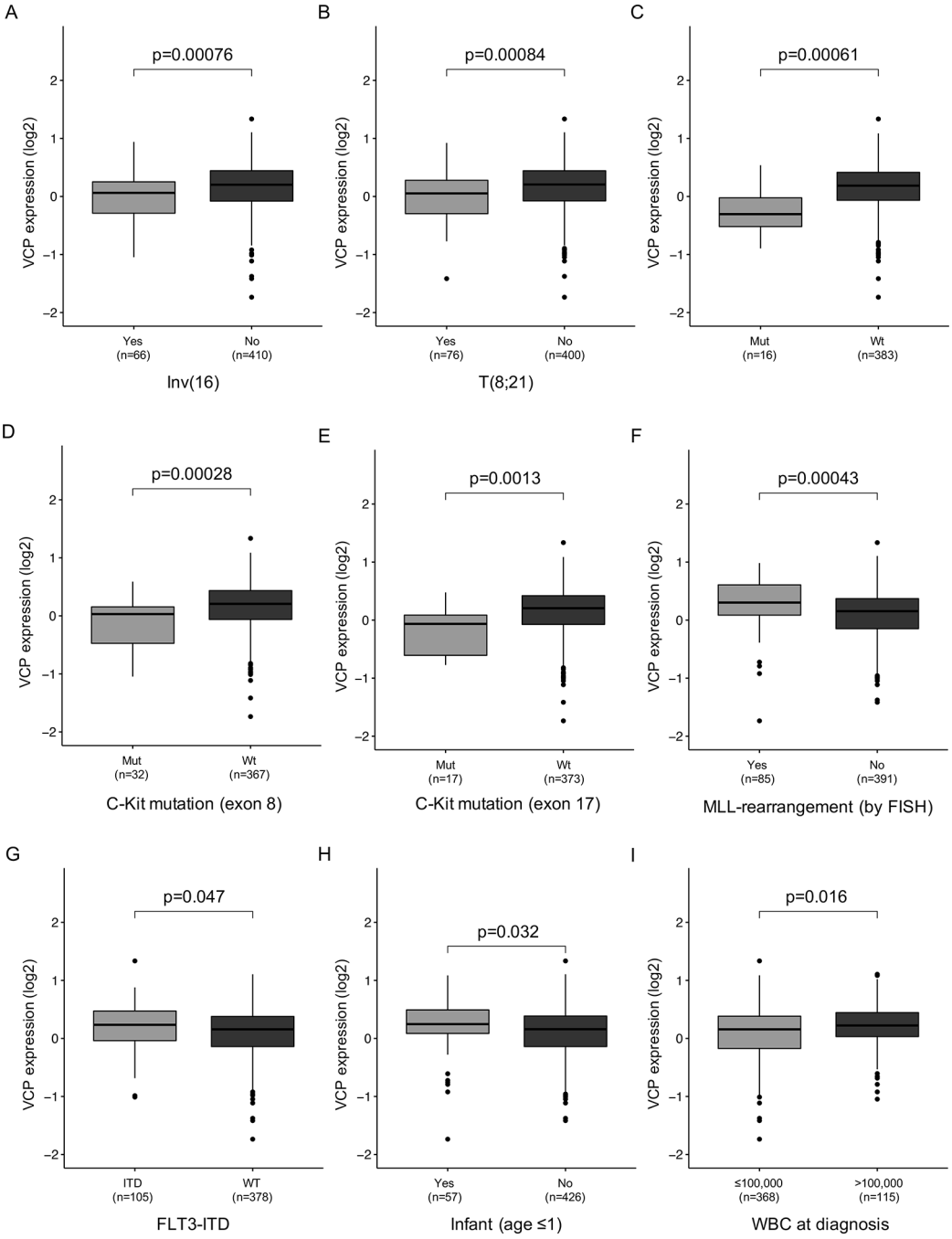

Figure 1. RPPA protein expression levels for the 483 de novo pediatric AML patients for VCP-total.

Boxplots represent the dispersion of VCP expression across different genetic molecular subgroups: **A**, inversion 16, **B**, translocation 8;21, **C**, C-kit mutation (exon 8), **D**, C-kit mutation (exon 17), **E**, MYH11 mutation, **F**, MLL-rearrangement (KMT2A), **G**, FLT3-ITD, **H**, infants (patients age ≤ 1) and **I**, white blood cell count at diagnosis. Wilcoxon Signed Rank test was used to compare mean values of the molecular subgroups.

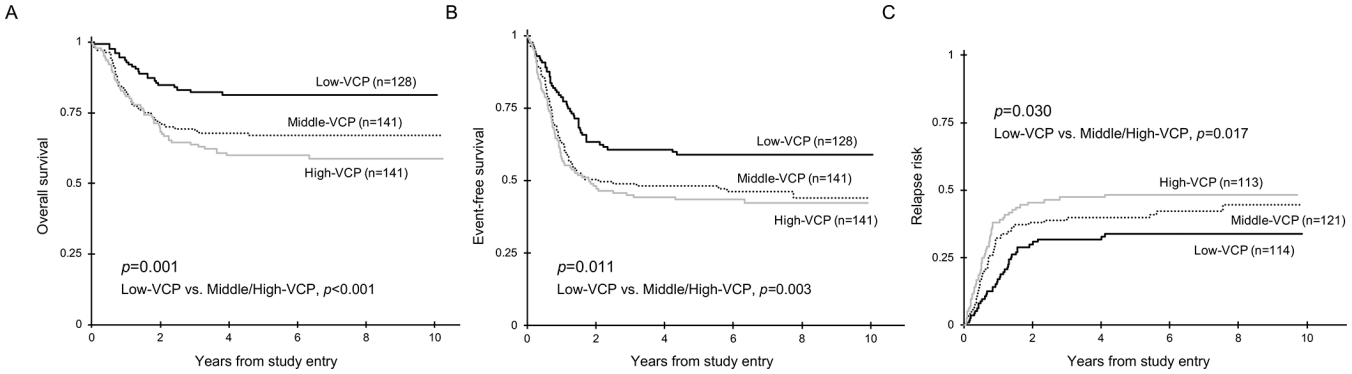

Figure 2. Kaplan-Meier survival curves for overall survival, event-free survival and relapse risk.

A) Overall survival, **B)** event-free survival and **C)** relapse risk for patients stratified based on their relative VCP levels. Black solid lines (—) indicate low-VCP patients, dotted (....) lines represent middle-VCP and gray solid lines (—) the high-VCP patients. P-values are calculated across the three groups, as well as across the low-VCP vs middle/high-VCP patients. Differences between groups of patients were tested for significance using the log-rank statistic for OS and EFS and using the Gray's test for RR.

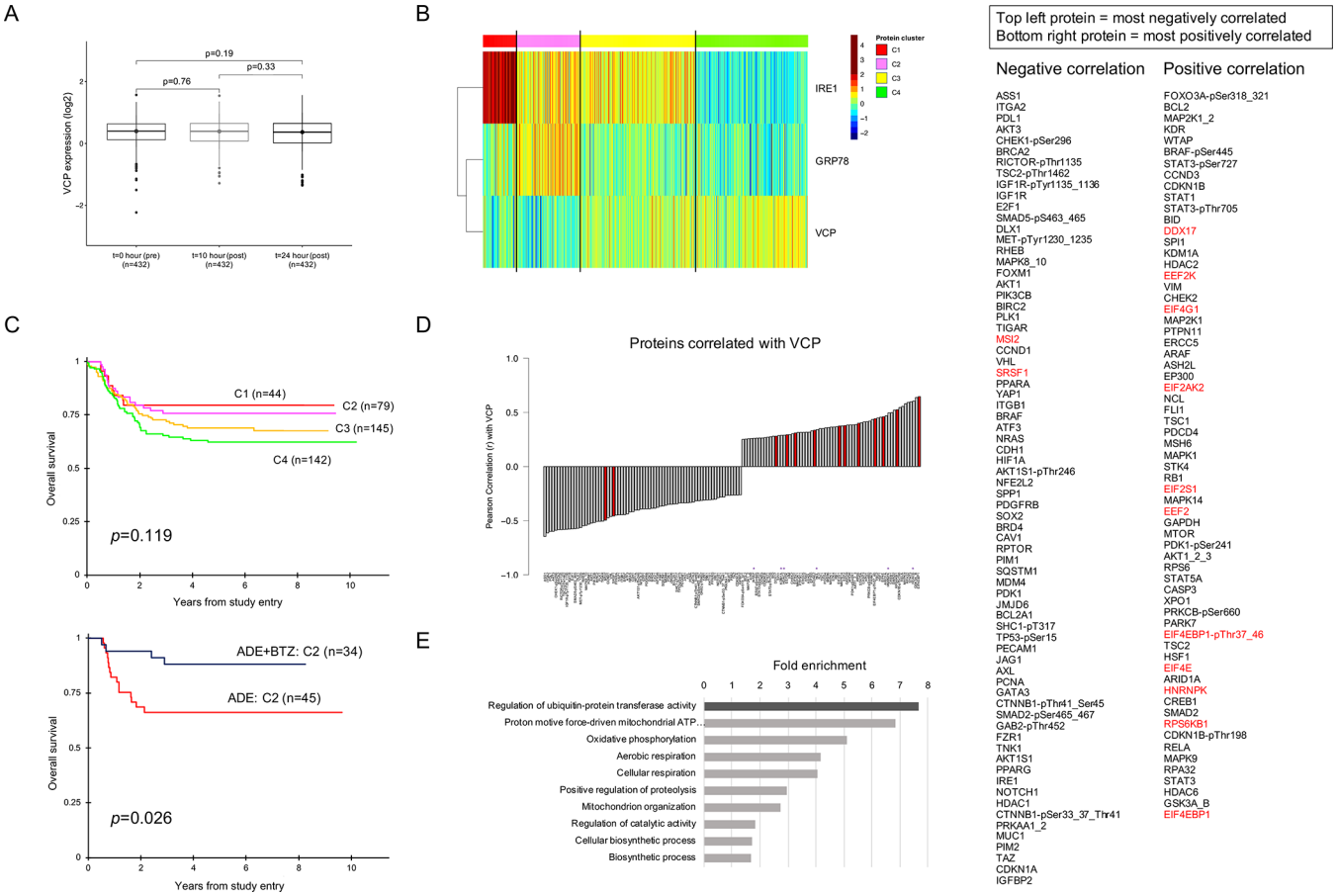

Figure 3.

A, change in VCP protein expression following chemotherapy. This figure shows the change in VCP expression following chemotherapy over time between 432 paired pediatric AML patient samples. Wilcoxon Signed Rank test was used to compare mean values of the molecular subgroups. **B**, heat map showing relative proteins expression levels for the 483 patients for IRE1, GRP78 and VCP. The Progeny Clustering algorithm (coupled with k-means) was performed and identified four proteins clusters (C1, C2, C3, C4). The colors reflect the median expression levels relative to the 20 normal CD34+ samples. Proteins expressed greatly below normal are shown as dark blue, and proteins expressed significantly above normal are shown in dark red (maroon). Proteins within the range of the normal cells are colorized in green (extended up to yellow and down to aqua). Each column represents a single patient. The annotation bar shows patient membership for the different protein clusters [C1 (red), C2 (magenta), C3 (yellow), and C4 (light green)]. **C**, Kaplan-Meier overall survival analysis for the four identified protein clusters (upper panel) and well as for patients that form protein cluster two treated with ADE (red) vs ADEB (navy blue). Differences between groups of patients were tested for significance using the log-rank statistic for OS. **D**, list of proteins significantly correlated with VCP protein expression (Pearson's correlation coefficient ≥ 0.25 or ≤ −0.25). Proteins shown in red are involved in initiation or elongation of protein translation or in ribosomal processes, protein denoted with a asterisk at involved in histone modification. Magnified version of the protein names is

shown on the right. **E**, differentially expressed genes between patients with low-VCP protein expression levels and middle/ high-VCP. Top 10 of biological processes associated with most fold enrichment based on gene ontology enrichment analysis is shown.

Table 1.

Patient's characteristics (n=483)

	Type	Freq. (%)	Low-VCP	Middle-VCP	High-VCP	*p*
Number	Count	100%	33%	33%	33%	
Gender	Female	50%	53%	47%	50%	0.569
Age	≤ 1 yo	12%	7%	11%	17%	0.033
	2–10 yo	55%	60%	57%	50%	0.936
	> 11 yo	33%	33%	32%	34%	0.175
Ethnicity †	Hispanic	19%	22%	16%	19%	0.383
CNS involvement	Positive	39%	33%	41%	43%	0.175
WBC at study entry	>100000	24%	16%	29%	27%	0.019
Risk stratification (AAML1031) ‡	High risk	28%	24%	24%	35%	0.046
Cytogenetics	t(8;21)	16%	20%	17%	10%	0.031
	Inv(16)/t(16;16)	14%	20%	13%	8%	0.008
	t(9;11)(p22;q23)/11q23	18%	11%	16%	25%	0.003
	Normal	28%	23%	31%	29%	0.252
	+8, -5, -7	9%	7%	10%	10%	0.528
	Other abnormalities	15%	16%	12%	17%	0.339
	Unknown	1%	2%	1%	1%	-
NPM1-mutation	Mutated	10%	9%	11%	11%	0.855
CEBPα-mutation	Mutated	9%	6%	12%	9%	0.144
FLT3-ITD	ITD	22%	18%	20%	27%	0.100
c-Kit (Exon 8)	Mutated	4%	10%	1%	1%	0.000
c-Kit (Exon 17)	Mutated	8%	12%	9%	4%	0.048
NRAS	Mutated	25%	30%	27%	19%	0.130
KRAS	Mutated	7%	6%	8%	8%	0.654
PTPN11	Mutated	7%	7%	5%	9%	0.514
MYH11	Mutated	4%	7%	5%	1%	0.031
IDH1 or 2	Mutated	4%	3%	5%	3%	0.764
GATA2	Mutated	3%	2%	2%	5%	0.197
MRD (at end of induction II)	Positive	22%	22%	15%	30%	0.009

	Type	Freq. (%)	Low-VCP	Middle-VCP	High-VCP	*p*
Response	Complete remission	78%	78%	81%	75%	0.096

Unknown values were not considered in P value calculations and are excluded from the results.

[†]N=3 patients have unknown ethnicity and are excluded from the results.

[‡]AAML1031 protocol risk group definition: low risk, inv(16)/t(16;16) or t(8;21), or NPM1 or CEBPα mutation; high risk, FLT3/ITD with high allelic ratio≥0.4, or monosomy 5/del5q or 7, without low-risk features; and risk status unknown for 14 of 483.

Table 2.

Multivariable analysis

		OS from study entry				EFS from study entry			RR from end of course 2			
		N	**HR**	**95% CI**	**p**	**HR**	**95% CI**	**p**	**N**	**HR**	**95% CI**	**p**
VCP	Low	126	1			1			114	1		
	Middle	138	1.96	1.17 – 3.29	0.010	1.47	1.02 – 2.10	0.038	121	1.40	0.93 – 2.13	0.111
	High	136	2.11	1.28 – 3.49	0.004	1.47	1.03 – 2.11	0.036	113	1.72	1.13 – 2.63	0.011
Risk group (AAML1031 definition)	Low	281	1			1			265	1		
	High	119	2.55	1.74 – 3.74	<0.001	1.75	1.29 – 2.36	<0.001	83	1.08	0.72 – 1.61	0.717
Age (years old)	2–10	135	1			1			119	1		
	0–1	46	2.28	1.33 – 3.92	0.003	2.31	1.51 – 3.54	<0.001	37	1.72	1.02 – 2.90	0.043
	11+	219	0.97	0.64 – 1.46	0.883	0.86	0.63 – 1.18	0.358	192	0.73	0.50 – 1.04	0.083